



Synthesis, characterization, and DNA-binding of enantiomers of iron(II) Schiff base complexes

Zhi-Guo Gu^{a,b,*}, Jing-Jing Na^a, Fei-Fei Bao^a, Xin-Xin Xu^a, Wen Zhou^a, Chun-Yan Pang^a, Zaijun Li^a

^a School of Chemical and Material Engineering, Jiangnan University, Wuxi 214122, PR China

^b Coordination Chemistry Institute and the State Key Laboratory of Coordination Chemistry, School of Chemistry and Chemical Engineering, Nanjing University, Nanjing 210093, PR China

ARTICLE INFO

Article history:

Received 23 October 2012

Accepted 21 December 2012

Available online 7 January 2013

Keywords:

Schiff base

Iron(II) complexes

Enantiomers

DNA binding

Enantioselectivity

ABSTRACT

Two pairs of iron(II) chiral enantiomers *fac*- Δ -[Fe(S-L1)₃][ClO₄]₂ and *fac*- Λ -[Fe(R-L1)₃][ClO₄]₂ (Δ -**1** and Λ -**1**), *fac*- Δ -[Fe(S-L2)₃][ClO₄]₂ and *fac*- Λ -[Fe(R-L2)₃][ClO₄]₂ (Δ -**2** and Λ -**2**), L1 = (*R/S*)-(±)-1-naphthyl-N-(pyridine-2-ylmethylene)ethanamine, L2 = (*R/S*)-(±)-2-naphthyl-N-(pyridine-2-ylmethylene)ethanamine were synthesized and characterized by elemental analysis, IR, UV–Vis, CD and ¹H NMR spectra. The X-ray structural analyses of Λ -**1** and Δ -**2** revealed that the iron(II) complexes possess octahedral coordination geometry for N6 donor atoms by three bidentate ligands. *R*-L1 ligand induces the *fac*- Λ isomer, while *S*-L2 ligand induces the *fac*- Δ isomer. The enantioselective binding of iron(II) chiral enantiomers to calf-thymus DNA (ct-DNA) has been investigated by methods of UV–Vis, fluorescence, and circular dichroism spectrometry. All the complexes could bind to ct-DNA and showed different binding affinities with the binding constants ranging from 0.91×10^5 to 1.43×10^5 M⁻¹. Moreover, the Δ enantiomers exhibited more efficient DNA interaction with respect to the Λ enantiomers.

© 2013 Elsevier Ltd. All rights reserved.

1. Introduction

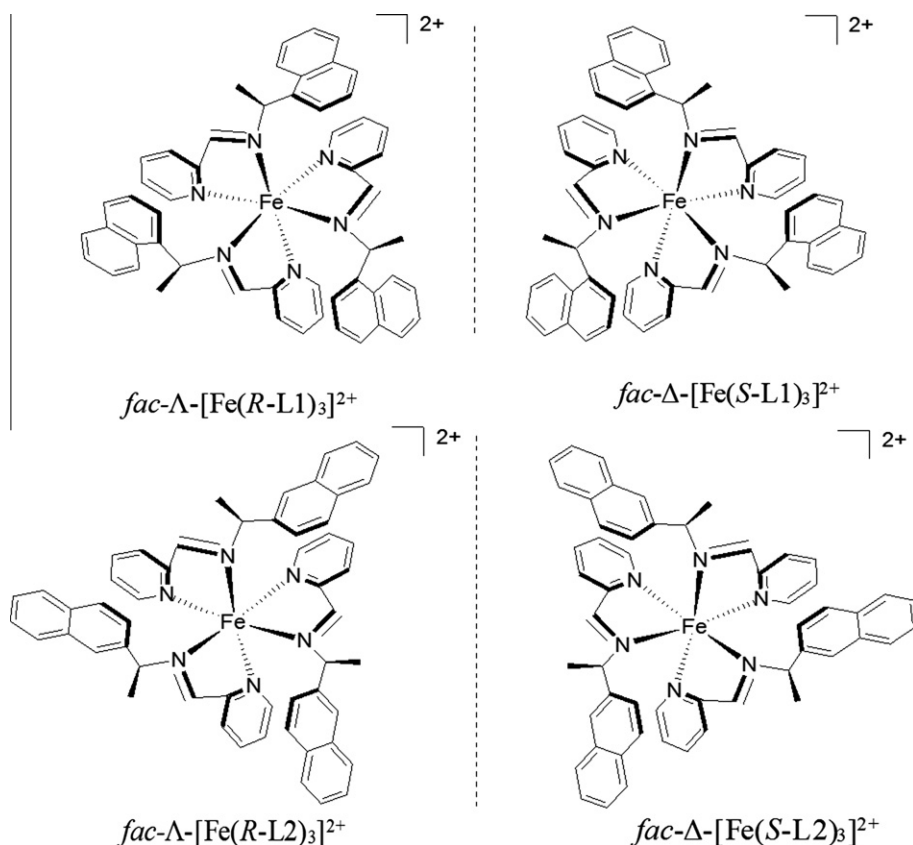
In the past few decades, small molecule transition metal complexes that can interact with DNA have attracted much attention in the field of bioinorganic chemistry [1–5]. In particular, octahedral polypyridyl transition metal complexes with extended aromatic heterocyclic ligands have been used extensively as DNA structural probes, DNA molecular light-switch, DNA electron transfer, DNA cleaving reagents and potential anti-cancer drugs [6–10]. Chiral recognition of DNA is crucial for developing structural probes of DNA conformation and rational drug design. Since natural B-form DNA with right-handed double helix is inherently chiral, its interactions with chiral metal complexes should be, in principal diastereoselective [11]. This was indeed observed in particular chiral propeller-like octahedral complexes with two possible conformations, i.e. the left-handed (Λ) and the right-handed (Δ) enantiomers [12–17]. However, determination of optical purity of octahedral metal complexes was challenging, and separation by diastereomeric crystallization or chromatographic techniques has inherently low yields [18]. Recently, Muggers' group introduced a

straightforward and economical asymmetric synthesis of nonracemic ruthenium(II) polypyridyl complexes based on using the readily available starting material together with chiral auxiliary [19,20].

In order to develop new homochiral octahedral metal complexes fitting the right-handed DNA and to explore their enantioselectivity, we focused on tris(diimine) iron(II) complexes which present a variety of possible isomers (Δ and Λ , *fac* and *mer*). Our strategies employed include the use of rational designed enantiopure unsymmetrical ligand by which chiral information can be transferred to the metal centre [21]. In this way, a predetermination of the absolute configuration at the metal centre can be reached [22]. We report here the assembly of optically pure, single diastereomer *fac*-tris(diimine) Fe(II) complexes *fac*- Δ -[Fe(S-L1)₃][ClO₄]₂ and *fac*- Λ -[Fe(R-L1)₃][ClO₄]₂ (Δ -**1** and Λ -**1**), *fac*- Δ -[Fe(S-L2)₃][ClO₄]₂ and *fac*- Λ -[Fe(R-L2)₃][ClO₄]₂ (Δ -**2** and Λ -**2**), by introducing optically pure (*R/S*)-(±)-1-naphthyl-N-(pyridine-2-ylmethylene)ethanamine or (*R/S*)-(±)-2-naphthyl-N-(pyridine-2-ylmethylene)ethanamine as ligands (Scheme 1), and the detailed results of enantioselective studies on the ct-DNA binding of the iron(II) complexes. It is interesting that complexes **1** with 1-naphthyl groups have stronger DNA binding ability than complexes **2** with 2-naphthyl groups, and the Δ -enantiomer exhibited more efficient DNA interaction with respect to the Λ -enantiomer.

* Corresponding author at: School of Chemical and Material Engineering, Jiangnan University, Wuxi 214122, PR China. Tel.: +86 510 85917090; fax: +86 510 85917763.

E-mail address: zhiguogu@jiangnan.edu.cn (Z.-G. Gu).



Scheme 1. The molecular structures of chiral Schiff base Fe(II) complexes.

2. Experimental

2.1. Materials and methods

Calf thymus DNA (ct-DNA) was purchased from Sino-American Biotechnology Co., Ltd. (*R/S*)-(±)-1-naphthyl-N-(pyridine-2-ylmethylene)ethanamine, (*R/S*)-(±)-2-naphthyl-N-(pyridine-2-ylmethylene)ethanamine, $\text{Fe}(\text{ClO}_4)_2 \cdot 6\text{H}_2\text{O}$, 2-pyridinecarboxaldehyde, and ethidium bromide (EB) were purchased from Sigma–Aldrich and used as received. All other reagents and solvents were purchased from commercial sources and used without further purification. Ultrapure water ($18.2 \text{ M}\Omega \text{ cm}$) was used in all experiments. The solution of DNA was prepared in 5 mM tris(hydroxymethyl)methanamin–HCl (Tris–HCl) buffer with 50 mM NaCl, pH 7.2, and all DNA experiments were conducted in this buffer solution. Given the ratio of UV absorbance at 260 and 280 nm, $A_{260}/A_{280} = 1.9$, the DNA was sufficiently free of protein [23]. The DNA concentration (represented by molar concentration of bases pairs) was determined spectroscopically by using the molar extinction coefficient at the maximum of the long wavelength absorbance: $\epsilon = 6600 \text{ cm}^{-1} \text{ mol}^{-1} \text{ dm}^3$. Concentration of stock solutions of the metal complexes were 10^{-3} M in acetonitrile. *fac*-[*Fe*(*R/S*-L1)₃][ClO_4]₂·CH₃CN **1** and *fac*-[*Fe*(*R/S*-L2)₃][ClO_4]₂·2CH₃CN **2** were synthesized as described below. ¹H NMR spectra were recorded on AVANCE III (400 MHz) instrument at 298 K using standard Bruker software. The spectra were internally referenced using the residual protio solvent resonance relative to tetramethylsilane ($\delta = 0 \text{ ppm}$). Infrared spectra were measured on an ABB Bomem FTLA 2000–104 spectrometer with KBr pellets in the 400–4000 cm^{-1} region. Element analyses were conducted on elemental corporation vario EL III analyzer. Circular dichroism (CD) spectra was carried out using a MOS-450/AF-CD spectropolarimeter at room temperature, which was

calibrated conventionally using 0.060% ACS for intensity and a holmium filter for wavelength.

2.2. Synthesis of *fac*-[*Fe*(*R/S*-L1)₃][ClO_4]₂·CH₃CN and *fac*-[*Fe*(*R/S*-L2)₃][ClO_4]₂·2CH₃CN

A mixture of 2-pyridinecarboxaldehyde (0.064 g, 0.6 mmol) and (*R/S*)-(1-naphthyl)ethylamine or (*R/S*)-(2-naphthyl)ethylamine (0.100 g, 0.6 mmol) dissolved in 30 mL acetonitrile was refluxed for 3 h. After the mixture cooled to room temperature, $\text{Fe}(\text{ClO}_4)_2 \cdot 6\text{H}_2\text{O}$ (0.073 g, 0.2 mmol) was added, and the solution turned purple immediately. The solution was stirred overnight before diethyl ether was added dropwise until signs of crystallization. The purple crystals were filtered and dried under vacuum. The complexes were recrystallized from acetonitrile by slow diffusion of anhydrous ether. All the complexes are stable and nonhygroscopic in air at room temperature. The complexes were highly soluble in MeOH, DMSO, MeCN, slightly soluble in water, acetone and EtOH.

2.2.1. *fac*-Λ-[*Fe*(*R*-L1)₃][ClO_4]₂·CH₃CN (**A-1**)

Purple crystalline solid (68%): IR (KBr cm^{-1}): $\nu = 3444 \text{ (w)}$, 2975 (w), 2936 (w), 2360 (w), 2341 (w), 1638 (s), 1379 (m), 1113 (w), 1088 (s), 760 (s), 703 (m), 620 (s); ¹H NMR (400 MHz, $(\text{CD}_3)_2\text{SO}$ δ ppm): 8.634 (s, 1H, H–C=N), 8.553 (d, $J = 10.8 \text{ Hz}$, 1H, Py), 8.319 (d, $J = 8.4 \text{ Hz}$, 1H, Py), 8.068 (m, 1H, Py), 7.960 (m, 1H, Py), 7.890–7.760 (broad m, 3H, naph), 7.644–7.450 (broad m, 4H, naph), 5.535 (q, $J = 7.5 \text{ Hz}$, 1H, C–H), 1.665 (d, $J = 6.4 \text{ Hz}$, 3H, CH₃); *Anal.* Calc. for $\text{C}_{56}\text{H}_{51}\text{Cl}_2\text{FeN}_7\text{O}_8$: C, 62.46; N, 9.11; H, 4.77. Found: C, 62.31; N, 9.02; H, 4.86%. UV–Vis λ_{max} : 569, 519, 333, 280 nm. CD (nm): 593 (negative), 522 (positive), 361 (positive), 323 (negative), 285 (positive).

2.2.2. *fac-Λ-[Fe(S-L1)]3[ClO4]2·CH3CN (Λ-1)*

Purple crystalline solid (63%): IR (KBr cm^{-1}): $\nu = 3428$ (w), 2968 (w), 2924 (w), 2367 (w), 2335 (w), 1638 (s), 1379 (m), 1120 (w), 1088 (s), 765 (s), 712 (m), 620 (s); $^1\text{H NMR}$ (400 MHz, $(\text{CD}_3)_2\text{SO}$ δ ppm): 8.634 (s, 1H, H–C=N), 8.553(d, $J = 10.8$ Hz, 1H, Py), 8.319 (d, $J = 8.4$ Hz, 1H, Py), 8.068 (m, 1H, Py), 7.960 (m, 1H, Py), 7.890–7.760 (broad m, 3H, naph), 7.644–7.449 (broad m, 4H, naph), 5.533 (q, $J = 7.5$ Hz, 1H, C–H), 1.665 (d, $J = 6.4$ Hz, 3H, CH_3); *Anal.* Calc. for $\text{C}_{56}\text{H}_{51}\text{Cl}_2\text{FeN}_7\text{O}_8$: C, 62.46; N, 9.11; H, 4.77. Found: C, 62.28; N, 9.06; H, 4.91%. UV–Vis λ_{max} : 569, 519, 333, 280 nm. CD (nm): 593 (positive), 522 (negative), 361 (negative), 323 (positive), 285 (negative).

2.2.3. *fac-Λ-[Fe(R-L2)]3[ClO4]2·2CH3CN (Λ-2)*

Purple crystalline solid (72%): IR (KBr cm^{-1}): $\nu = 3474$ (w), 2943 (w), 2926 (w), 2329 (w), 2287 (w), 1608 (s), 1379 (m), 1113 (w), 1088 (s), 759 (s), 696 (m), 620 (s); $^1\text{H NMR}$ (400 MHz, $(\text{CD}_3)_2\text{SO}$ δ ppm): 8.629 (s, 1H, H–C=N), 8.550(d, $J = 10.4$ Hz, 1H, Py), 8.320 (d, $J = 8.4$ Hz, 1H, Py), 8.067 (m, 1H, Py), 7.959 (m, 1H, Py), 7.907–7.759 (broad m, 3H, naph), 7.642–7.451 (broad m, 4H, naph), 5.533 (q, $J = 7.6$ Hz, 1H, C–H), 1.665 (d, $J = 6.4$ Hz, 3H, CH_3); *Anal.* Calc. for $\text{C}_{58}\text{H}_{54}\text{Cl}_2\text{FeN}_8\text{O}_8$: C, 62.32; N, 10.02; H, 4.87. Found: C, 62.18; N, 9.87; H, 4.95%. UV–Vis λ_{max} : 568, 519, 341, 279 nm. CD (nm): 590 (negative), 515 (positive), 358 (positive), 313 (negative), 286 (positive).

2.2.4. *fac-Λ-[Fe(S-L2)]3[ClO4]2·2CH3CN (Λ-2)*

Purple crystalline solid (74%): IR (KBr cm^{-1}): $\nu = 3468$ (w), 2975 (w), 2954 (w), 2322 (w), 2265 (w), 1608 (s), 1379 (m), 1113 (w), 1088(s), 752(s), 698(m), 620(s); $^1\text{H NMR}$ (400 MHz, $(\text{CD}_3)_2\text{SO}$ δ ppm): 8.630 (s, 1H, H–C=N), 8.551(d, $J = 10.4$ Hz, 1H, Py), 8.320 (d, $J = 8.4$ Hz, 1H, Py), 8.067 (m, 1H, Py), 7.959 (m, 1H, Py), 7.907–7.757 (broad m, 3H, naph), 7.642–7.451 (broad m, 4H, naph), 5.533 (q, $J = 7.6$ Hz, 1H, C–H), 1.665 (d, $J = 6.4$ Hz, 3H, CH_3); *Anal.* Calc. for $\text{C}_{58}\text{H}_{54}\text{Cl}_2\text{FeN}_8\text{O}_8$: C, 62.32; N, 10.02; H, 4.87. Found: C, 62.15; N, 9.91; H, 4.99%. UV–Vis λ_{max} : 568, 519, 341, 279 nm. CD (nm): 590 (positive), 515 (negative), 358 (negative), 313 (positive), 286 (negative).

2.3. X-ray crystallography

The crystal structures were determined on a Bruker APEX-II diffractometer with a CCD area detector at 298 K with Mo $\text{K}\alpha$ radiation ($\lambda = 0.71073$ Å). Cell parameters were retrieved using SMART software and refined using SAINT [24] on all observed reflections. Data were collected using a narrow-frame method with scan widths of 0.30° in ω and an exposure time of 10s/frame. The highly redundant data sets were reduced using SAINT [24] and corrected for Lorentz and polarization effects. Absorption corrections were applied using SADABS [25] supplied by Bruker. Structures were solved by direct methods using the program SHELXS-97 [26]. The positions of metal atoms and their first coordination spheres were located from direct-methods *E*-maps; other non-hydrogen atoms were found in alternating difference Fourier syntheses and least-squares refinement cycles and, during the final cycles, refined anisotropically. Hydrogen atoms were placed in calculated position and refined as riding atoms with a uniform value of U_{iso} . Final crystallographic data and values of R_1 and wR are listed in Table 1. Relevant bond distances and angles are listed in Table 2.

2.4. DNA-binding studies

2.4.1. Absorption spectroscopy

The stock solution of chiral Schiff base iron(II) complexes in acetonitrile (1 mM) were used for spectroscopic titration of DNA solution in Tris–HCl buffer (5 mM, 50 mM NaCl, pH 7.2), by keeping the

Table 1

Summary of crystallographic data for the complexes Λ -1 and Δ -2.

	Λ -1	Δ -2
Formula	$\text{C}_{56}\text{H}_{51}\text{Cl}_2\text{FeN}_7\text{O}_8$	$\text{C}_{58}\text{H}_{54}\text{Cl}_2\text{FeN}_8\text{O}_8$
Formula weight	1076.79	1117.84
Crystal system	cubic	triclinic
Space group	$P2_13$	$P1$
<i>a</i> (Å)	17.370(2)	11.689(3)
<i>b</i> (Å)	17.370(2)	11.845(3)
<i>c</i> (Å)	17.370(2)	12.183(3)
α ($^\circ$)	90	106.183(5)
β ($^\circ$)	90	110.174(4)
γ ($^\circ$)	90	107.910(5)
<i>V</i> (Å ³)	5240.9(12)	1359.6(5)
<i>Z</i>	4	1
<i>D</i> _{calc} (g cm ⁻³)	1.365	1.365
<i>T</i> (K)	298(2)	298(2)
μ (mm ⁻¹)	0.452	0.439
θ ($^\circ$)	1.66–27.52	2.00–25.10
<i>F</i> (000)	2240	582
Index ranges	$-19 \leq h \leq 22$, $-21 \leq k \leq 22$, $-22 \leq l \leq 18$	$-9 \leq h \leq 13$, $-14 \leq k \leq 12$, $-14 \leq l \leq 14$
Data/restraints/ parameters	3962/8/223	5995/1580/697
Goodness-of-fit (GOF) on (<i>F</i> ²)	0.881	1.019
R_1^a , wR_2^b ($I > 2\sigma(I)$)	0.0489, 0.1133	0.0750, 0.1789
R_1^a , wR_2^b (all data)	0.0792, 0.1225	0.0978, 0.2224
Flack <i>X</i>	0.01(3)	0.00(2)

^a $R_1 = \sum ||F_o| - |F_c|| / \sum F_o$.

^b $wR_2 = [\sum w(F_o^2 - F_c^2)^2 / \sum w(F_o^2)]^{1/2}$.

Table 2

Selected bond lengths (Å) and angles ($^\circ$) for Λ -1 and Δ -2.

Λ -1			
Fe(1)–N(1)	1.971(3)	Fe(1)–N(2)	1.998(3)
N(1A)–Fe(1)–N(2)	91.60(11)	N(1A)–Fe(1)–N(1)	92.14(12)
N(1)–Fe(1)–N(2)	81.45(12)	N(2A)–Fe(1)–N(2)	95.16(11)
Δ -2			
Fe(1)–N(4)	1.954(9)	Fe(1)–N(1)	1.972(7)
Fe(1)–N(2)	1.974(8)	Fe(1)–N(3)	1.987(8)
Fe(1)–N(5)	1.991(9)	Fe(1)–N(6)	1.991(8)
N(4)–Fe(1)–N(1)	92.3(3)	N(4)–Fe(1)–N(2)	94.7(3)
N(1)–Fe(1)–N(2)	81.0(3)	N(4)–Fe(1)–N(3)	81.1(3)
N(1)–Fe(1)–N(3)	94.6(3)	N(3)–Fe(1)–N(6)	91.0(3)
N(4)–Fe(1)–N(6)	96.5(3)	N(1)–Fe(1)–N(5)	92.0(3)
N(2)–Fe(1)–N(6)	94.0(3)	N(3)–Fe(1)–N(5)	92.2(3)
N(2)–Fe(1)–N(5)	92.2(3)	N(6)–Fe(1)–N(5)	79.7(3)

Symmetry codes: $A z + 1/2, -x + 3/2, -y + 1$.

concentration of acetonitrile as 1% throughout the experiments. Accordingly, incremental quantity of DNA solution from 0 to 84 μM was added to the fixed concentration of metal complex solution 30 μM , NaCl and Tris–HCl buffer concentrations remained constant. UV–Vis absorbance spectra were collected on Shimadzu UV-2101 PC scanning spectrophotometer.

2.4.2. Ethidium bromide (EB) fluorescence competition binding assay

The fluorescence spectra recorded in Tris–HCl buffer of the complex concentration was incrementally increased from 0 to 30 μM while keeping the concentrations of DNA (80 μM) and EB (4 μM) constant. Fluorescence spectra were collected on a Shimadzu RF-5301 spectrofluorometer with excitation at 528 nm, excitation slit 5.0 and emission slit 5.0 nm. The emission spectra were recorded at 550–700 nm.

2.4.3. Circular dichroism spectroscopy

The circular dichroism (CD) titration series was carried out using a MOS-450/AF-CD spectropolarimeter at room temperature with the fixed concentration constant at 30 μM of the chiral metal complexes. The baseline was subtracted from Tris-HCl buffer (5 mM, 50 mM NaCl, pH 7.2) for each data set. By adding equal volumes of the concentrated DNA solution to the 1 cm path length flow cell, the DNA:metal complex ratios are 1:6, 1:3, 1:2, 2:3, 1:1, respectively. Each CD spectrum has been subtracted by free DNA thus the spectrum purely reflect the changes in the enantiomer of the complex upon binding DNA.

3. Results and discussion

3.1. Synthesis and characterization

The diamagnetic tris-pyridine/imine Schiff base Fe(II) complexes were prepared by a one-pot strategy, mixing iron(II) perchlorate hexahydrate into a solution of the appropriate chiral naphthylethylamine and 2-pyridinecarboxaldehyde in acetonitrile. This led to the immediate formation of intense purple solutions, from which the perchlorate salt crystals could be readily obtained with high yields by diffusion of anhydrous ether. The complexes **1** and **2** were characterized by various spectroscopic and analytical techniques. Solid IR spectroscopic analysis revealed intense absorptions at 1638 for **1** and 1608 cm^{-1} for **2**, due to the $\nu_{\text{C}=\text{N}}$ stretching vibration of the Schiff base ligands at room temperature, while peaks at 1088 and 620 cm^{-1} revealed the existence of ClO_4^- . UV-Vis spectra for all the complexes show the absorption bands for coordinated ligand at 280 nm, and the characteristic MLCT transition at 568 nm. The CD spectra of Δ -**1** and Λ -**1**, Δ -**2** and Λ -**2** are mirror images of each other which contain intense features spanning the whole UV-Vis region, demonstrating their absolute configuration and enantiopurity. The ^1H NMR spectra for all the iron(II) complexes showed only one set of coordinated ligand signals, hence a single diastereoisomer with a C_3 -symmetric *fac* structure is formed. Take Λ -**2** as an example, it showed doublet at 1.665 for the CH_3 protons, quartet at 5.533 for CH proton, singlet at 8.629 for H-C=N proton. The protons of pyridine appeared at 8.550–7.959, the multiplet at 7.907–7.759 and 7.642–7.451 are belonging to the seven protons of naphthalene. Extensive overlapping of the ^1H signals in the aromatic region renders complete spectral assignment difficult.

To further confirm the structures of the chiral Schiff base Fe(II) complexes, the crystal structures of Λ -**1** and Δ -**2** were determined. X-ray crystallography revealed that Λ -**1** and Δ -**2** crystallized in the chiral space groups $P2_13$ and $P1$, respectively. The two structures both consist of one $[\text{Fe}(\text{L})_3]^{2+}$ cation, two perchlorate counterions, and uncoordinated acetonitrile molecules (Figs. 1 and 2). The Fe(II) sites with N_6 coordination environments in Λ -**1** and Δ -**2** both form distorted octahedral geometries. The average iron–nitrogen bond lengths of 1.984(5) for Λ -**1** and 1.978(1) for Δ -**2** are consistent with the low-spin state at 298 K [27]. The three unsymmetrical ligands in Λ -**1** and Δ -**2** mount a face of the octahedron designating a *fac* arrangement, in which each of the three pyridine units forms an intramolecular π – π stacking interaction with a naphthyl unit on a neighboring ligand. The average centroid-to-centroid distances are 3.997 Å and 3.558 Å, and the average angles between arene planes are 16.441° and 5.932° for Λ -**1** and Δ -**2**, respectively. These parallel-displaced π – π interactions of the rings could account for the extraordinary stereoselectivity for the *fac* structures observed in Λ -**1** and Δ -**2**. Comparable π – π stacking effects have been observed between the pyridine group and the phenyl ring in the *fac*-Fe(II) complexes with diimine ligands derived from 2-iminopyridine and (*R*)-2-phenylglycinol derivatives [21]. The octahedral cations

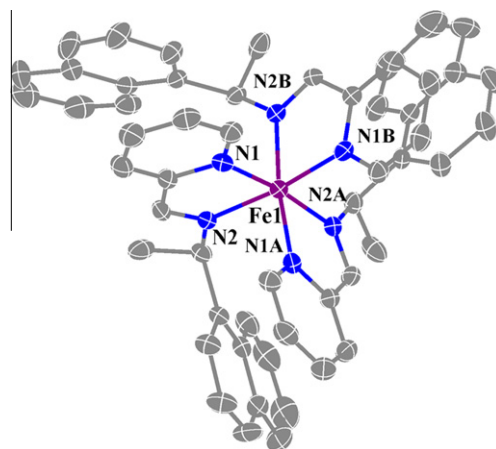


Fig. 1. Structure of the cation in the asymmetric unit of *fac*- Λ - $[\text{Fe}(\text{R-L1})_3][\text{ClO}_4]_2 \cdot 2\text{CH}_3\text{CN}$ (Λ -**1**) with thermal ellipsoids are shown at 30% probability. H atoms, counterions and solvent molecules omitted for clarity. (Symmetry codes: A $z + 1/2, -x + 3/2, -y + 1$; B $-y + 3/2, -z + 1, x - 1/2$.)

$[\text{Fe}(\text{R-L1})_3]^{2+}$ and $[\text{Fe}(\text{S-L2})_3]^{2+}$ adopt exclusively Λ and Δ form, respectively. It seems that the stereochemically active groups of the ligands orient the configuration of the overall complexes, where the ligands transfer their chirality to the metal centre, preventing the classical racemization of Λ/Δ species [22]. The cations of Λ -**1** and Δ -**2** pack through weak T-shaped C–H $\cdots \pi$ contacts between the phenyl groups, resulting in the formation of three-dimensional supramolecular structures with channels filled with ClO_4^- anions and acetonitrile molecules.

3.2. DNA binding experiments

3.2.1. Electronic absorption spectroscopy

UV-Vis spectroscopy is the most useful technique in DNA-binding studies [28]. Hypochromism and red shift are usually observed when a complex binds to DNA. The extent of the hypochromism commonly parallels the binding strength. Fig. S1 and Table 3 show the results of the UV-Vis spectroscopy of the complexes Δ -**1**, Λ -**1**, Δ -**2** and Λ -**2** titrated against DNA at a constant complexes concentration of 30 μM . All complexes showed some extent of hypochromism by increasing DNA concentrations from 0 to 84 μM . Meanwhile, different complexes with different chirality

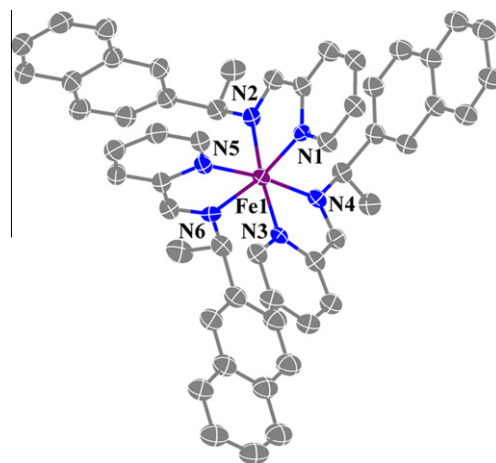


Fig. 2. Structure of the cation in the asymmetric unit of *fac*- Δ - $[\text{Fe}(\text{S-L2})_3][\text{ClO}_4]_2 \cdot 2\text{CH}_3\text{CN}$ (Δ -**2**) with thermal ellipsoids are shown at 30% probability. H atoms, counterions and solvent molecules omitted for clarity.

Table 3The data for UV–Vis titration of complexes Λ -1, Δ -1, Λ -2, and Δ -2 against DNA.

Complexes	λ_{\max} (free) (nm)	λ_{\max} (bound) (nm)	$\Delta\lambda$ (nm)	Hypochromism (%)
Λ -1	569 258	572 259	3 1	16.9
Δ -1	569 258	572 258	3 0	17.3
Λ -2	569 258	570 258	1 0	8.2
Δ -2	569 258	569 258	0 0	10.1

Table 4Binding constant of complexes Λ -1, Δ -1, Λ -2, and Δ -2.

Complexes	Hypochromism (%)	λ_{\max} (DNA + EB)	λ_{\max} (DNA + EB + complexes)	K	$K_{\text{app}}/10^5$ (M^{-1})
Λ -1	55.9	600	607	3.40 ± 0.045	1.11
Δ -1	64.6	603	609	4.87 ± 0.015	1.43
Λ -2	51.8	600	607	2.87 ± 0.015	0.91
Δ -2	52.5	600	607	2.96 ± 0.021	0.98

caused varying changes in their electronic absorption spectroscopy. The bands around 569 nm of iron(II) metal \rightarrow ligand charge transfer (MLCT) displayed minor red shift and hypochromism, indicating mainly groove binding mode instead of intercalative. When the chiral mononuclear iron(II) complexes with two positive charges bind with DNA in the groove, the negative charges on the phosphates of the DNA backbone will be neutralized. Therefore, the structure of DNA becomes loosen or collapse at the binding area, and the configuration of DNA shows some extent of bending or distortion [29,30]. The hypochromic rates at λ_{\max} (free) of enantiomers are showed in Table 3. Interestingly, among all the complexes we studied, the Δ -enantiomers had better binding efficiency than their Λ -enantiomers.

3.2.2. Ethidium bromide fluorescence competition binding assay

The ethidium bromide (EB) displacement assay was usually used to determine Stern–Volmer constant of the complex to bind DNA particularly when the complex failed to show any luminescence upon excitation of CT and LMCT band. In the present study, the solutions of chiral complexes Δ -1, Λ -1, Δ -2, and Λ -2 in different solvents did not show any luminescence irrespective of the presence and absence of DNA. Therefore, EB which is known to emit intense fluorescence in the presence of DNA due to the strong intercalation of EB between the base pairs of DNA was used as a spectral probe [31]. The EB competition assay was carried out for each complex with the concentrations of DNA and EB being constant. The intense fluorescence obtained by the interaction of EB and DNA got diminished by the addition of chiral iron(II) Schiff

base complexes (Fig. S2). This might be due to the displacement of EB by bivalent metal complex cations results from charge neutralization on the DNA backbone, which is accompanied by a part of collapse of linear DNA. The EB insert in this area deviated from the base pair [32]. Moreover, the binding equilibrium of EB towards the solution phase shifted, which is confirmed by the change of peak data of luminescence [33] (peak data see Table 4).

Based on Fig. S2, the Stern–Volmer constants were calculated by using following functional equation [34]:

$$I_0/I = 1 + K \cdot r \quad (1)$$

In the above equation I_0 and I are the emission intensities in the absence and presence of metal complexes; r is the ratio of the total concentration of chiral metal complexes to DNA; and K is the Stern–Volmer quenches constant. The apparent binding constants (K_{app}) for enantiomers are calculated from $K_{\text{EB}} \times [\text{EB}] = K_{\text{app}} \times [\text{drug}]$, where $[\text{EB}]$ is the concentration of EB ($4 \mu\text{M}$); $[\text{drug}]$ is the concentration of chiral metal compounds at a 50% reduction of fluorescence; and K_{EB} is known ($K_{\text{EB}} = 1.3 \times 10^6 \text{M}^{-1}$ for ct-DNA) [35]. The data were shown in Table 4. The results of fluorescence experiment are in accordance with the UV/vis titration results presented above. The values of K are sufficiently large to conclude that in the experiments reported herein all the iron(II) metal complexes can bind to DNA, and the qualitative ranking of the DNA binding strength is Δ -1 > Λ -1 > Δ -2 > Λ -2.

3.2.3. Circular dichroism spectroscopy

CD is the difference in absorption of left and right circularly polarized light, and is uniquely sensitive to any asymmetric interaction such as that between the chiral DNA and the chiral metal complex. Therefore it has been utilized as a powerful tool for providing valuable information on the mode of binding between DNA helix and chiral complexes [36,37]. The changes in intrinsic CD of chiral complexes reflect the binding geometry and binding mode of the complexes as well as the DNA bases. The CD spectra of Δ -1 and Λ -1, Δ -2 and Λ -2 enantiomers are expected mirror images of one another. With increasing addition of ct-DNA, the CD spectra of Δ -1, Λ -1, Δ -2, and Λ -2 recorded from 400 to 650 nm (MLCT region) are shown in Fig. 3. Compared with the absorption spectra, the CD spectra showed dramatic distinction in the bond strength between the different compounds upon addition of ct-DNA. In the MLCT wavelength region the decreases in intensity for Δ -1 and Λ -1 enantiomers are apparent, while the changes of Δ -2 and Λ -2 are comparatively slight. This indicates complexes **1** have better interaction with DNA than complexes **2** due to their special structures that can bind DNA in groove more suitable. With increasing DNA, the MLCT region band is more perturbed in the case of Δ -enantiomer. This suggests that the

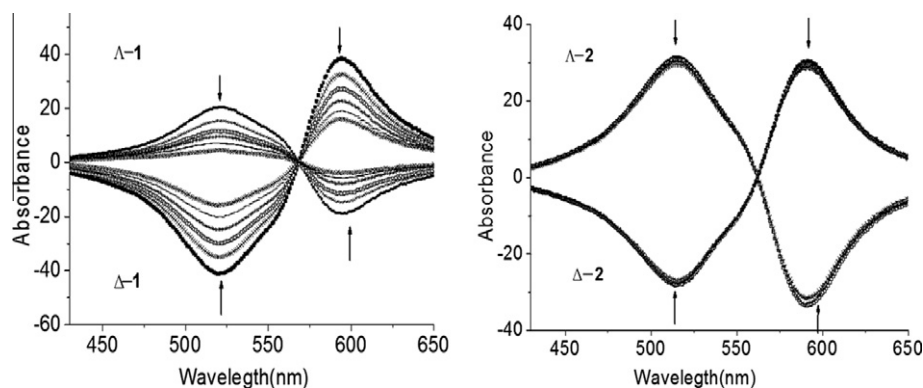


Fig. 3. The CD spectral profiles developing in the MLCT region upon the binding of Δ -1, Λ -1, Δ -2, Λ -2 ($30 \mu\text{M}$) to ct-DNA in the presence of increasing concentration of ct-DNA (0 – $30 \mu\text{M}$), pathlength 1 cm (400–650 nm).

Δ -enantiomer interacts more strongly with DNA, compared to the Λ -isomer. For the Δ -enantiomer, the right-handed propeller-like structure with appropriate steric matching with right-handed ct-DNA displays a greater affinity than the Λ -enantiomer.

4. Conclusion

Two pairs of mononuclear iron(II) chiral enantiomers with Schiff base ligands were synthesized with good yields by convenient procedures. The complexes possess octahedral geometry of absolute configuration in solution and solid state. The ligand chirality plays a crucial role in determining the geometrical isomerism of the possible *fac*- and *mer*-isomers and enantiomorphism of the possible Δ - and Λ -enantiomers. The DNA binding behaviors of the chiral complexes have been investigated by UV absorption, fluorescence, and circular dichroism spectrometry. Results suggest that all complexes can interact with DNA and the binding mode with DNA may most likely to be the groove binding mode. Interestingly, discernible differences of enantiomeric selectivity have been observed in the interaction of the different enantiomers with DNA. The Δ -enantiomer of the complexes showed stronger DNA binding ability than the Λ -enantiomer, suggesting that the Δ isomer has restricted mobility when bound to DNA because it is more deeply buried in the groove of DNA compared to the Λ isomer. The details of the DNA binding mode, specific binding sites and enantiomeric selectivity are not very clear at present and further studies are currently in progress.

Acknowledgments

This work was supported by the National Natural Science Foundation of China (21101078 and 21276105), the Program for New Century Excellent Talents in University of China (NCET-11-0657), and the Natural Science Foundation of Jiangsu Province (BK2011143), the Fundamental Research Funds for the Central Universities (JUSRP21111), the State Key Laboratory of Coordination Chemistry of Nanjing University.

Appendix A. Supplementary material

CCDC 894297 and 894298 contain the supplementary crystallographic data for Λ -1 and Δ -2. These data can be obtained free of charge via <http://www.ccdc.cam.ac.uk/conts/retrieving.html>, or from the Cambridge Crystallographic Data Centre, 12 Union Road, Cambridge CB2 1EZ, UK; fax: (+44) 1223 336 033; or e-mail: deposit@ccdc.cam.ac.uk. Supplementary data associated with this

article can be found, in the online version, at <http://dx.doi.org/10.1016/j.poly.2012.12.027>.

References

- [1] K.E. Erkkila, D.T. Odom, J.K. Barton, *Chem. Rev.* 99 (1999) 2777.
- [2] C. Metcalfe, J.A. Thomas, *Chem. Soc. Rev.* 32 (2003) 215.
- [3] M.J. Hannon, *Chem. Soc. Rev.* 36 (2007) 280.
- [4] F.R. Keene, J.A. Smitha, J.G. Collins, *Coord. Chem. Rev.* 253 (2009) 2021.
- [5] M.R. Gill, J.A. Thomas, *Chem. Soc. Rev.* 41 (2012) 3179.
- [6] U. McDonnell, M.R. Hicks, M.J. Hannon, A. Rodger, *J. Inorg. Biochem.* 102 (2008) 2052.
- [7] J.K. Barton, E.D. Olmon, P.A. Sontz, *Coord. Chem. Rev.* 255 (2011) 619.
- [8] H.K. Liu, P.J. Sadler, *Acc. Chem. Res.* 44 (2011) 349.
- [9] J.D. Aguirre, A.M. Angeles-Boza, A. Chouai, J.P. Pellois, C. Turro, K.R. Dunbar, *J. Am. Chem. Soc.* 131 (2009) 11353.
- [10] C.J. Burrows, J.G. Muller, *Chem. Rev.* 98 (1998) 1109.
- [11] R. Corradini, S. Sforza, T. Tedeschi, R. Marchelli, *Chirality* 19 (2007) 269.
- [12] J.K. Barton, *Science* 233 (1986) 727.
- [13] H. Song, J.T. Kaiser, J.K. Barton, *Nat. Chem.* 4 (2012) 615.
- [14] S.E. Howson, A. Bolhuis, V. Brabec, G.J. Clarkson, J. Malina, A. Rodger, P. Scott, *Nat. Chem.* 4 (2012) 31.
- [15] J.K. Barton, L.A. Basile, A. Danishefsky, A. Alexandrescu, *Proc. Natl. Acad. Sci. USA* 81 (1984) 1961.
- [16] H.J. Yu, X.H. Wang, M.L. Fu, J.S. Ren, X.G. Qu, *Nucleic Acids Res.* 36 (2008) 5695.
- [17] Mudasir, N. Yoshioka, H. Inoue, *J. Inorg. Biochem.* 102 (2008) 1638.
- [18] S. Torelli, S. Delahaye, A. Hauser, G. Bernardinelli, C. Piguet, *Chem. Eur. J.* 10 (2004) 3503.
- [19] L.A. Chen, J.J. Ma, M.A. Celik, H.L. Yu, Z.X. Cao, G. Frenking, L. Gong, E. Meggers, *Chem. Asian J.* 7 (2012) 2523.
- [20] C. Fu, M. Wenzel, E. Treutlein, K. Harms, E. Meggers, *Inorg. Chem.* 51 (2012) 10004.
- [21] S.E. Howson, L.E.N. Allan, N.P. Chmel, G.J. Clarkson, R.J. Deeth, A.D. Faulkner, D.H. Simpson, P. Scott, *Dalton Trans.* 40 (2011) 10416.
- [22] J. Crassous, *Chem. Soc. Rev.* 38 (2009) 830.
- [23] M.E. Reichmann, S.A. Rice, C.A. Thomas, P. Doty, *J. Am. Chem. Soc.* 76 (1954) 3047.
- [24] SAINT-Plus, version 6.02, Bruker Analytical X-ray System, Madison, WI, 1999.
- [25] G.M. Sheldrick, SADABS An Empirical Absorption Correction Program, Bruker Analytical X-ray Systems, Madison, WI, 1996.
- [26] G.M. Sheldrick, *Acta Crystallogr., Sect. A* 64 (2008) 112.
- [27] A.G. Orpen, L. Brammer, F.H. Allen, O. Kennard, D.G. Watson, R. Taylor, *J. Chem. Soc., Dalton Trans.* (1989) S1.
- [28] J.K. Barton, A.T. Danishefsky, J.M. Goldberg, *J. Am. Chem. Soc.* 106 (1984) 2172.
- [29] V.A. Bloomfield, *Biopolymers* 44 (1997) 269.
- [30] N. Korolev, N.V. Bereznoy, K.D. Eom, J.P. Tam, L. Nordenskiöld, *Nucleic Acids Res.* 37 (2009) 7137.
- [31] B. Maity, M. Roy, S. Saha, A.R. Chakravarty, *Organometallics* 28 (2009) 1495.
- [32] X.D. Dong, X.Y. Wang, Y.F. He, Z. Yu, M.X. Lin, C.L. Zhang, J. Wang, Y.J. Song, Y.M. Zhang, Z.P. Liu, Y.Z. Li, Z.J. Guo, *Chem. Eur. J.* 16 (2010) 14181.
- [33] A.L.M. Le Ny, C.T. Lee, *Biophys. Chem.* 142 (2009) 76.
- [34] S.K. Teo, W.A. Colburn, W.G. Tracewell, K.A. Kook, D.I. Stirling, M.S. Jaworsky, M.A. Scheffler, S.D. Thomas, O.L. Laskin, *Clin. Pharmacokinet.* 43 (2004) 311.
- [35] M.D. Wyatt, B.J. Garbiras, M.K. Haskell, M. Lee, R.L. Souhami, J.A. Hartley, *Anti-Cancer Drug Des.* 1 (1994) 511.
- [36] B. Peng, W.H. Zhou, L. Yan, H.W. Liu, L. Zhu, *Transition Met. Chem.* 34 (2009) 231.
- [37] R. Vijayalakshmi, M. Kanthimathi, R. Parthasarathi, B.U. Nair, *Bioorg. Med. Chem.* 14 (2006) 3300.